GAS TEMPERATURE MEASUREMENTS USING THE DUAL-LINE DETECTION RAYLEIGH SCATTERING TECHNIQUE*

M. Volkan Otugen
Polytechnic University
Brooklyn, NY

Richard G. Seasholtz
NASA Lewis Research Center
Cleveland, OH

Kurt D. Annen
Aerodyne Research, Inc.
Billerica, MA

SUMMARY

A new laser-induced Rayleigh scattering method is presented for the improved temperature diagnostics of gas flows. In the present technique, the two lines of a copper vapor laser are used to obtain the time and space resolved temperature. A single set of optics is used to form the optical probe and to collect the signal simultaneously from both the 510 nm and the 578 nm lines. The dual-line detection allows for the determination and removal of surface-scattered laser light from a Rayleigh signal thereby improving the applicability of Rayleigh scattering to near wall flows with a high degree of glare. An optical system using the dual-line detection technique is built, calibrated and tested in a hot air jet under various levels of background contamination. The results indicate that highly accurate temperature measurements are possible even when the laser-line background intensity, captured by the collecting optics, is five times that of the Rayleigh signal.

NOMENCLATURE

C optical system calibration constant

C' surface scattering calibration constant

---

* Work was undertaken at NASA Lewis Research Center

I_B surface scattered background intensity
I_L laser light intensity
I_R Rayleigh signal intensity
I_T total intensity captured by collecting optics
I_0 Incident light intensity
k Loschmidt number
L irradiated length of sample
n gas number density
P gas pressure
R gas constant
T temperature
α gas index of refraction
β ratio of surface scattering constants
θ scattering angle
λ wavelength of laser light
σ' standard deviation
σ Rayleigh scattering cross-section
X mean value

Subscripts

1 refers to the 510 nm line
2 refers to the 578 nm line

INTRODUCTION

Rayleigh scattering is an optical technique which has been successfully used as a temperature and concentration measurement tool in fluid dynamics and combustion research. For example, Graham et al. (1974), Dyer (1979), Pitts and Kashiwagi (1984) and Arcoumanis (1985) measured tracer concentration in non-reacting, binary gas jets while Otugen and Namer (1988) measured temperature in a non-isothermal air jet. The technique has also been applied to simple reacting flows. Bill et al. (1982) and Gouldin and Halthore (1986) measured total gas density while Dibble and Hollenbach (1981) and Namer and Shefer (1985) measured flame temperatures, all in premixed external flames using laser induced Rayleigh scattering. Temperature measurements have also been attempted in combustors (eg. Barat et al., 1991) but these have had limited success due to signal contamination by laser glare. During the last few years, there have been attempts to use Rayleigh scattering for two-dimensional imaging of density and concentration both in subsonic jets (Escoda and Long, 1983) and supersonic wind tunnel

testing (Smith et al, 1989; Shirinizadeh et al., 1991). However, high speed wind tunnel applications for density diagnostics have remained mostly qualitative due to the unwanted scattering of laser light from ice cluster and surrounding surfaces. On the other hand, the application of spectrally resolved Rayleigh scattering as supersonic flow anemometry has been quite successful when the flow velocities are high enough to produce a clearly detectable Doppler shift in scattered signal (Seasholtz, 1991).

A commonly encountered difficulty associated with the Rayleigh scattering technique is the contamination of the relatively low level of Rayleigh signal by the background noise. The two major sources of background noise are the contribution of light from the test environment, which is usually broadband, and the surface scattered laser glare captured by the collecting optics along with the Rayleigh signal. Since the Rayleigh line scattered from the gas molecules in the probe have approximately the same central frequency as the laser beam, surface scattered light cannot be easily discriminated from Rayleigh scattering, especially in low speed flows. In certain applications, particularly in enclosed flows with limited optical access such as combustors, surface scattered glare can become a formidable obstacle . The problem becomes most severe when near forward or near backward collecting angles have to be used, since scattering from surfaces and optical elements are larger at these angles.

In the present study, different methods are used to minimize the effects of both types of background contamination. A pulsed copper-vapor laser with a repetition rate of 6 kHz and a continuous output power of 20 watts is used as the light source. The use of a pulsed source provides a comparatively high level of Rayleigh signal due to the high energy densities at each pulse and greatly suppresses the effect of environmental noise. However, the improved pulse energy does not help increase the ratio of signal-to-background due to laser glare. A new dual-line detection technique is developed to address this problem. The signal is collected from both the 510 nm (green) and the 578 nm (yellow) lines of the copper-vapor laser using one set of collecting optics. The information obtained from both lines is analyzed together at each shot of the laser to determine the laser line background level and to decouple it from the Rayleigh signal. The dual-line detection method eliminates the need for the guesswork in background determination and offsetting and significantly improves the potential of Rayleigh scattering as a reliable quantitative diagnostic tool in high temperature gas flows including combustion.

An optical system at NASA Lewis Research Center is used to test the dual-line detection technique. The dual-line detection Rayleigh (DLDR) system uses a copper-vapor laser as the light source. Optical fibers are used to transmit the laser beam to probe region and the signal to collecting optics. Extensive calibration tests have been performed to characterize the various system parameters. Finally, temperature measurements have successfully been performed in a heated air jet. Results indicate that highly accurate temperature measurements are possible using the dual-line detection in the presence of high level background glare. The method for background determination

is described in the following section.

DUAL-LINE BACKGROUND DETECTION

Rayleigh scattering involves the elastic interaction of the incident laser light with the gas molecules (Van de Hulst, 1957). The intensity of the scattered light is proportional to the incident laser light intensity, the scattering cross-section of the gas as well as the number density of the gas. Therefore, the technique can be used to measure density directly, or temperature, by invoking the ideal gas law. The intensity of Rayleigh scattered light by a unit volume of gas and an infinitesimal solid angle is given (Jenkins and White, 1981) by

$$I_R = I_o\, nL\sigma \tag{1}$$

Here, σ is the Rayleigh cross-section of the sampled gas and is a function of the scattering angle, θ , wavelength of incident beam, λ , and the index of refraction of gas, α. For an isotropic molecule, the Rayleigh cross-section can be expressed as follows:

$$\sigma = \frac{4\pi^2}{\lambda^4}\left(\frac{\alpha - 1}{k}\right)^2 sin^2\theta \tag{2}$$

where k is the Loschmidt number. For a multi-species gas volume the equivalent (average) cross-section can be found by the weighted average using the mole fraction of each species. Since the Rayleigh cross-section is proportional to -4 power of λ, laser lines with smaller wavelengths will result in a stronger signal for unit incident intensity. For a given experimental condition with a fixed collecting angle and laser line, the Rayleigh scattered light intensity can be written as

$$I_R = I_L C\sigma n \tag{3}$$

Here, I_L is the intensity of the laser light. The constant C absorbs all the parameters that are fixed for a given set-up. These parameters include the efficiency of the transmitting and collections optics, quantum efficiency of the photomultiplier, collection angle, solid angle over which signal is collected, amplification of electronic equipment, etc. However, as discussed above, the observed signal contains background due to surface scattered

laser glare as well as the Rayleigh signal so that

$$I_T = I_R + I_B = I_L \sigma n + I_L C C' \tag{4}$$

where, C' is a constant describing the surface scattering. Thus, the relative signal normalized by laser light intensity is

$$\frac{I_T}{I_L} = C\sigma \frac{P}{RT} + CC' \tag{5}$$

In the above equation, perfect gas law is used. For two line operation, Eq. (5) can be written for lines λ_1 and λ_2 (with $\lambda_1 = 510nm$ and $\lambda_2 = 578nm$, in the present case) as

$$\frac{I_{T,1}}{I_{L,1}} = C_1\sigma_1 \frac{P}{RT} + C_1C_1' \tag{6}$$

and

$$\frac{I_{T,2}}{I_{L,2}} = C_2\sigma_2 \frac{P}{RT} + C_2C_2' \tag{7}$$

For a given optical geometry and electronics setting the system can be calibrated to obtain the values for C_1, C_1', C_2 and C_2'. This can be accomplished by taking measurements under conditions where the values of σ, P and T are known and either one or a combination of these known quantities is varied. Therefore, a least squares fit of the data with a sufficient number of conditions will determine the constants C_1 and C_2, which are of importance. Furthermore, the ratio, $\beta = C_1' / C_2'$ is also obtained through the calibration process. It is reasonable to expect that the scattering process of light from solid surfaces at different wavelengths may be different. However, since the two beams (lines) from the laser are colinear, β should be a constant for a given system. As discussed later, this point is confirmed through experiments using the present DLDR system. Of course, $\beta = 1$ would indicate independence of surface scattering from the incident wavelength. With $C' = C_2'$ and $C_1' = \beta C'$, the following is obtained:

$$\frac{I_{T,1}}{I_{L,1}} = \left(\frac{C_1 P \sigma_1}{R}\right)\frac{1}{T} + \beta\, C_1 C' \tag{8}$$

$$\frac{I_{T,2}}{I_{L,2}} = \left(\frac{C_2 P \sigma_2}{R}\right)\frac{1}{T} + C_2 C' \tag{9}$$

Therefore, this linear system of two equations with unknowns 1/T and C' yields,

$$T = \frac{\frac{P}{R}(\sigma_1 - \beta\ \sigma_2)}{\frac{I_{T,1}}{I_{L,1}}\frac{1}{C_1} - \frac{I_{T,2}}{I_{L,2}}\frac{\beta}{C_2}} \tag{10}$$

and

$$C' = \frac{\frac{I_{T,2}}{I_{L,2}}\frac{\sigma_1}{C_2} - \frac{I_{T,1}}{I_{L,1}}\frac{\sigma_2}{C_1}}{(\sigma_1 - \beta\sigma_2)} \tag{11}$$

Equation (10) provides the temperature, decoupled from the background contamination. Obviously, this equation can be re-arranged for density if that property is desired in place of temperature. Equation (11) indicates the normalized background due to surface scattering at the laser lines at each measurement. This information is not related to flow physics; however, in practice, it will be of importance since its magnitude will determine if a particular measurement is reliable once a critical threshold value of signal-to-noise ratio is established from preliminary testing. Although Eqs. (10) and (11) completely decouple background from temperature, in practice, from optical and electronic considerations, there will be a limit on the signal-to-background ratio, specific to a DLDR system, below which an accurate measurement of temperature will not be possible. The present DLDR system was calibrated and tests have been performed to obtain such critical signal-to-noise values.

EXPERIMENTAL SYSTEM

The optical arrangement for the dual-line detection Rayleigh scattering system is shown in Fig 1. Central to the system is a pulsed copper-vapor laser with a continuous power output of about 20 watts. The laser is normally operated at a pulse rate of 6 kHz with a pulse duration of approximately 36 ns. The output beam contains both 510 nm (green) and the 578 nm (yellow) lines. The relative power of the 510 nm and the 578 nm lines are approximately 60 % and 40 %, respectively. The optical probe and the signal collecting optics are situated on an optical bench with a three-axis traverse capability. The laser is placed on a separate optical table and the output beam is transmitted to the

probe bench through an optical fiber. The beam is coupled into the 400 μm fiber by focusing it with a 150 mm focal length lens. The focussed beam first passes through a 600 0.6 mm pinhole for spatial filtering before reaching the cleaved fiber end. The fiber end is placed slightly beyond the minimum waist diameter location so that the fiber end is protected from burning under high incident laser energies. The transmitting optics are composed of two 150 mm focal length lenses producing a probe waist of about 400 μm. The incident power at the probe is approximately 1.4 watts although variations did occur on a day-to-day basis. The laser light is captured by a beam trap on the opposite side of the Rayleigh probe. Another light trap is situated directly behind the collecting optics to reduce the broadband background captured by the collecting optics. The collecting optics are comprised of two achromat lenses each with a 160 mm focal length and an 80 mm aperture. Therefore, the magnification factor of the collecting optics is unity. The collected signal is coupled into a 200 μm core diameter optical fiber and delivered into a sealed signal box. In the signal box, the total collected signal is collimated and subsequently color separated by a dielectric beam splitter. The green (510 nm) and the yellow (578 nm) signals are shined on two photomultiplier tubes.

Since the copper-vapor laser used has a significant pulse-to-pulse energy variation (up to 5 %), the intensity of the laser from two lines is monitored at each pulse and the signal is normalized by these values as required by Eqs. (8) and (9). This is accomplished by placing a thin glass plate at a small angle in front of the laser beam as shown in Fig. 1 and reflecting approximately ten percent of the beam energy. Some of the reflected laser light is then captured by the open end of a 200 μm core diameter fiber. At the other end of the fiber, this reference intensity is delivered to another box configured very similarly to the signal box. The only difference is that, the signal in the reference box is sensed by photodiodes instead of photomultiplier tubes.

The electronic arrangement for the DLDR system is shown in Fig. 2. The set of four sensor outputs for the two lines; the two signals from the photomultiplier tubes and the two laser reference intensities from the photodiodes are fed into linear gate and hold units on a boxcar averager system as shown. The signals from the photomultiplier tubes are fed directly to the gate integrators without any need for pre-amplification since a fairly strong Rayleigh signal is observed at each pulse of the laser. The timing for the gate generators is provided by a timing module. The timing module, which is a function generator with a TTL output, also provides the trigger pulses for the copper vapor laser and a 16 bit analog-to-digital converter. The trigger pulses to the gate generators and to the A/D converter are appropriately delayed to capture the Rayleigh scattering signal from the probe. The A/D converter is interfaced with an IBM 486 architecture personal computer. At each pulse of the laser, all four signals are gated, integrated, digitized and stored on the hard disk of a computer. Therefore, the system can obtain data at a rate of 6 kHz with a time resolution of about 36 ns. The data acquisition protocol is shown in Fig. 3. Data is post processed after each experiment or calibration on the same personal computer.

EXPERIMENTAL RESULTS

Preliminary tests were performed first to insure proper operation of the optical and the electronic components of the DLDR system for both the green, λ_1 and the yellow, λ_2 lines. Temperature was measured in a single, particulate free, heated air jet. For these measurements the dual-line detection feature was not implemented and temperature, independently measured from each laser line, was compared to a thermocouple measurement. Both the environmental background and the laser glare was kept to a minimum. For these measurements, the knowledge of the Rayleigh-cross section was not needed a priori. Each line was calibrated using a reference condition (free air jet at room condition) which is the usual method in the more conventional applications of Rayleigh scattering (eg. Dyer, 1979; Otugen and Namer, 1988). The optical probe was situated on the axis of a jet, approximately 1 mm above the nozzle (10 mm diameter). A chromel-alumel thermocouple with a nominal bead diameter of 1 mm was placed directly above the Rayleigh probe. Readings from both the Rayleigh scattering system and the thermocouple were obtained at various jet temperatures. Figure 4 shows a typical set of results. In the figure, a straight line with a slope of one is also drawn for better comparison. There is good agreement between the thermocouple and the Rayleigh scattering measurements. The slightly higher temperature readings independently obtained by both lines of the Rayleigh system are most likely due to the positioning of the thermocouple relative to the optical probe: The optical probe was slightly closer to the jet exit.

Two separate softwares were developed for the DLDR system: one for calibration and another for actual temperature measurements. The system has to be calibrated each time an experiment is performed since the constants in Eq. (8) and (9) are highly dependent on optical alignment and electronic settings (laser power, pmt sensitivity, electronic gain, gate width on signal integration, etc). Once the calibration procedure is completed, the related constants are put in the data acquisition software. At this point, any change on the electronics setting, including significant electronic drift would invalidate the calibration.

System Calibration

To qualify the DLDR system, a large set of calibration tests were performed under a diverse set of conditions related to both the optics and the electronics including the laser power, pmt sensitivities, signal gain, etc. Also, different levels of background were allowed to contaminate the signal during these tests to study the behavior of β . The calibration software essentially acquires data from both lines and performs a least squares fit to Eqs. (8) and (9). Values of σ, P and T are provided to the program and

depending on the experimental conditions, either one or a number of these parameters can be varied. In the present, the heated air jet previously mentioned was used. The Rayleigh scattering cross-sections and pressure (atmospheric) were provided to the software as fixed values and the air temperature was the calibration variable. The optical probe was placed at the exit of the jet and the jet temperature was varied. The temperature was monitored by a small-bead, chromel-alumel thermocouple which was placed adjacent to the optical probe.

A set of calibration graphs, performed during a day with various laser line contamination levels are shown in Fig. 5(a-d). The background contaminations were obtained by placing painted (flat black) and non-painted aluminum plates near the Rayleigh optical probe, directly opposite to the collecting optics (Fig. 1). Varying levels of background were obtained by moving the small, flat aluminum plates towards and away from the probe location on a traverse mechanism and allowing the diffuse laser light around the probe location to shine on the plates. The diffuse laser light, surrounding the high intensity beam waist (at the probe) is generated by the focussing lens. The pertinent values of the four constants obtained at each calibration are shown in the figures. The plots for both laser lines are linear confirming Eqs. (8) and (9). Also, for a given laser line, the slope of the plot is fixed for various background levels. Higher levels of background contamination simply lead to larger offset (y-intercept) in the plots. Furthermore, the values of C_1 and C_2 remain essentially constant throughout the experiments. The amount of fluctuation in these values is a measure of the accuracy of the calibration process. However, the most significant result here is the fact that, as postulated, $\beta = C_1' / C_2'$, remains nearly constant throughout the calibrations. Higher signal contamination by the surface scattered background leads to larger values of both C_1 and C_2. However, the ratio β remains nearly constant. The comparatively high value of β, obtained in Fig. 5(d) with the largest contamination level is believed to be related to the photomultiplier noise levels. A slightly higher background level than that corresponding to Fig. 5(d) led to the saturation of both photomultiplier tubes. This set a limit on the total acceptable signal. The results for the calibration constants, obtained for the same day are summarized in Table 1. The average value of β is 0.885 with a standard deviation of about 0.06. Note that these calibration results are obtained with nine data points on each calibration curve. A larger number of data points are likely to lead to lower standard deviation on the constants.

Temperature Measurements

Next, temperature was measured in a clean (particulate free) heated air jet with co-flow. Figure 6 shows the co-flow jet apparatus. The co-flow was added to the inner jet to prevent the entrainment of particulates from the laboratory environment. Excessive amounts of particulates in the probe region can prevent accurate measurements by contaminating the Rayleigh signal. Only the central jet is heated and jet exit

temperatures in excess of 800 K could be obtained with this jet apparatus. Again, a thermocouple was situated adjacent to the Rayleigh probe, on the downstream side. The thermocouple readings provide a comparison to the DLDR measurements.

Figure 7 shows the calibration results for the experiment. This time, the calibration is performed using 16 points. Since C_1 and C_2 depend on the electronic and optical settings, the current values are different than those previously obtained (Table 1). However, as expected, the value for β is almost identical to the average value previously obtained. In the figure, estimated error bars are also included at selected points.

The temperatures obtained by the DLDR system, approximately 2 mm above the exit plane, are shown in Figs. 8 and 9 for two jet heating levels. The solid line indicates the reading from the thermocouple. For a given heating level of the jet, multiples of DLDR measurements are obtained in the presence of various backgrounds. The background levels were created using the method previously described. For each contamination level, three records of temperature were obtained Each symbol in the figures represents the average value of a record (5128 samples per record). In these figures, a and b show the same temperature results against the signal-to-background ratio obtained from λ_1 and λ_2 lines, respectively. I_R / I_B ratios are obtained in the following manner: I_R is calculated from Eqs. (8) and (9), including only the first term on the right hand side and using the temperature reading from the thermocouple. I_B is obtained directly from the measurements using Eq. (11). The agreement between the DLDR and the thermocouple results is quite good. Particularly encouraging is the fact that even with signal-to-background levels as low as $I_{R,2}$ / $I_{B,2}$ = 0.2, reliable temperature measurements are possible. It should be noted that the lower limit on the signal-to-noise ratio that appears in Figs. 8 and 9 was determined by a practical consideration: beyond a certain position of the scattering surface, the background level increases sharply and saturates either the sensors or the electronic integrators rendering measurements impossible beyond that point.

CONCLUSIONS

A laser-induced Rayleigh scattering system is developed for gas temperature measurements. A dual-line detection technique is used for the effective detection and removal of the laser line glare from the Rayleigh signal. The technique involves the collection of signal from two lines of a laser. The two linear equations thus obtained are solved simultaneously to give temperature (or density) and the background level. In the present work, a pulsed copper vapor laser is used as the light source. The 510 nm and the 578 nm lines intrinsic to the laser provide the necessary two lines. The use of a pulsed laser greatly reduces the effect of broadband background from the surroundings. Calibration tests and actual temperature measurements also indicate that the dual-line

detection technique can improve the capability of Rayleigh scattering method by greatly reducing the effects of signal contamination due to laser glare. It eliminates the need for background mapping and the associated guesswork typical of Rayleigh scattering measurements in optically non-ideal situations. Accurate temperature measurements were obtained in a heated air jet even when the background level captured by the collecting optics was five times the Rayleigh signal. Using the dual-line detection technique, it is hoped that effective Rayleigh scattering measurements in enclosed test sections (such as in combustors with limited optical access) as well as near walls (such as in boundary layer studies) will be possible. Currently, a second DLDR system, similar to the one discussed here, is being developed which uses an Nd:YAG laser. In this new system, second and fourth harmonics of the laser output will be used as the two detection lines.

ACKNOWLEDGEMENTS

This work was undertaken while the first author was a summer faculty fellow at NASA Lewis Research Center, Optical Measurement Systems Branch. The support through NASA Grant NAG-3-1301 is also acknowledged.

REFERENCES

Arcoumanis, C.: A Laser Rayleigh Scattering System for Scalar Transport Studies. Exp. Fluids Vol.3, 1985 pp. 103-108.

Bill, R. G. Jr., Namer, I., Talbot, L., Robben, F.: Density Fluctuations of Flame in Grid Induced Turbulence. Combust. Flame, Vol. 44, 1982 pp.277-285.

Dibble, R.W.; and Hollenbach, R.E: Laser Rayleigh Thermometry in Turbulent Flows. Eighteenth Symposium on Combustion, 1981. The Combustion Institute pp. 1489-1499.

Dyer, T. M.: Rayleigh Scattering Measurements of Time-resolved Concentration in a Turbulent Propane Jet. AIAA J., Vol. 17, 1979 pp. 912-914.

Escoda,C.; and Long, M.B.: Rayleigh Scattering Measurements of Gas Concentration Field in Turbulent Jets. AIAA J., Vol 21, 1983, pp.81-84.

Gouldin, F.C.; and Halthore, R.N: Rayleigh Scattering for Density Measurements in Premixed Flames. Exp. Fluids, Vol. 4, 1986,pp. 269-278.

Graham, S.C.; Grant, A.J.; and Jones, J.M.: Transient Molecular Concentration Measurements in Turbulent Jets. AIAA J., Vol. 12, 1974, pp. 1140-1143.

Jenkins, F.A. and White, H.E.: Fundamentals of Optics, Fourth Edition. London, McGraw-Hill, 1981.

Namer, I. and Schefer, R.W.: Error Estimates for Rayleigh Scattering Density and Temperature Measurements. Exp. Fluids, Vol. 3 1985, pp. 1-9.

Otugen, M. V. and Namer, I.: Rayleigh Scattering Temperature Measurements in a Plane Turbulent Air Jet at Moderate Reynolds Numbers. Exp. Fluids, Vol. 6, 1988, pp. 461-466.

Pitts, W. M. and Kashiwagi, T.: The Application of Laser-induced Rayleigh Scattering to the Study of Turbulence Mixing. J. Fluid Mech. Vol. 141, 1984, pp.391-429.

Seasholtz,R.G.: High Speed Laser Anemometry Based on Spectrally Resolved Rayleigh Scattering. Proceedings of the Annual Conference on Laser Anemometry, August 5-9, 1991, Cleveland, OH.

Shirinzadeh, B; Hillard, M.E.; and Exton, R.J.: Condensation Effects on Rayleigh Scattering Measurements in Supersonic Wind Tunnel. AIAA J., Vol.29, 1991, pp.242-246.

Smith, M.; Smits, A.; and Miles, R.: Compressible Boundary Layer Density Cross Sections by UV Rayleigh Scattering. Optic Letters, Vol. 14, 1989, pp.916-918.

Van de Hulst, H. C.: Light Scattering by Small Particles. Chapmann & Hall, London 1957.

Table 1

	χ	σ'	σ' / χ
C_1	4.4248 E7	0.1545 E7	0.035
C_2	1.0479 E8	0.0361 E8	0.034
β	0.885	0.060	0.068

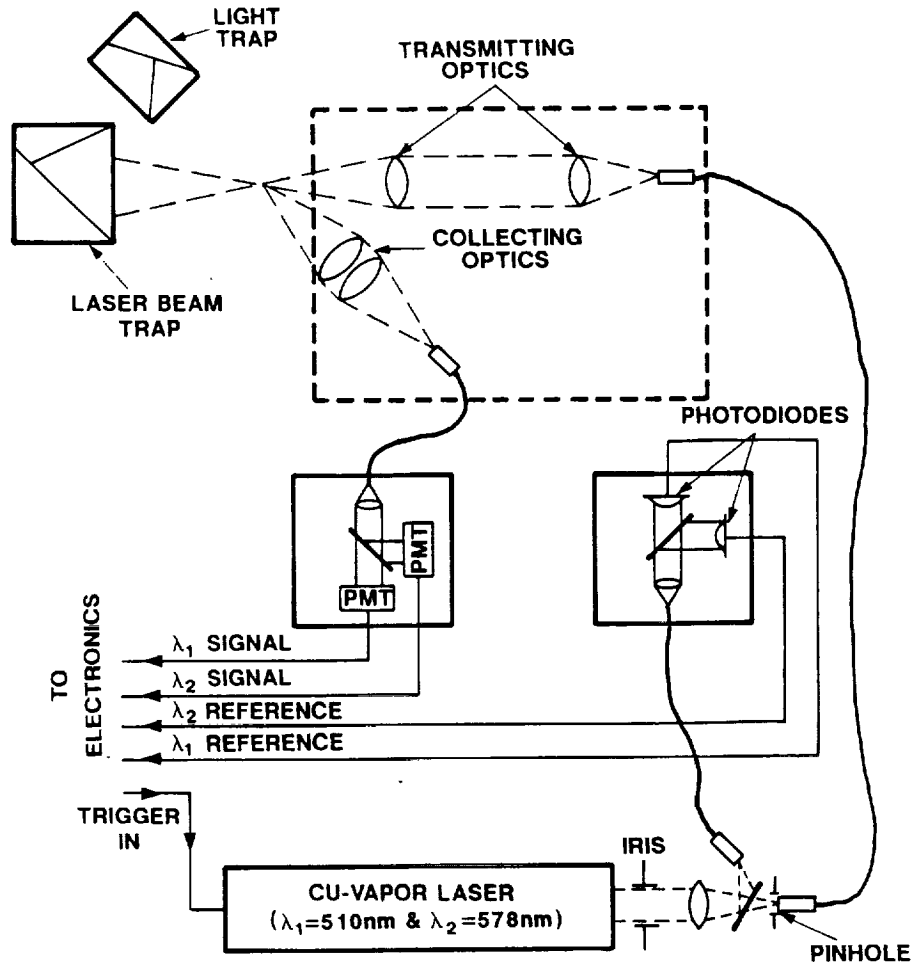

1. Optical arrangement for the DLDR system

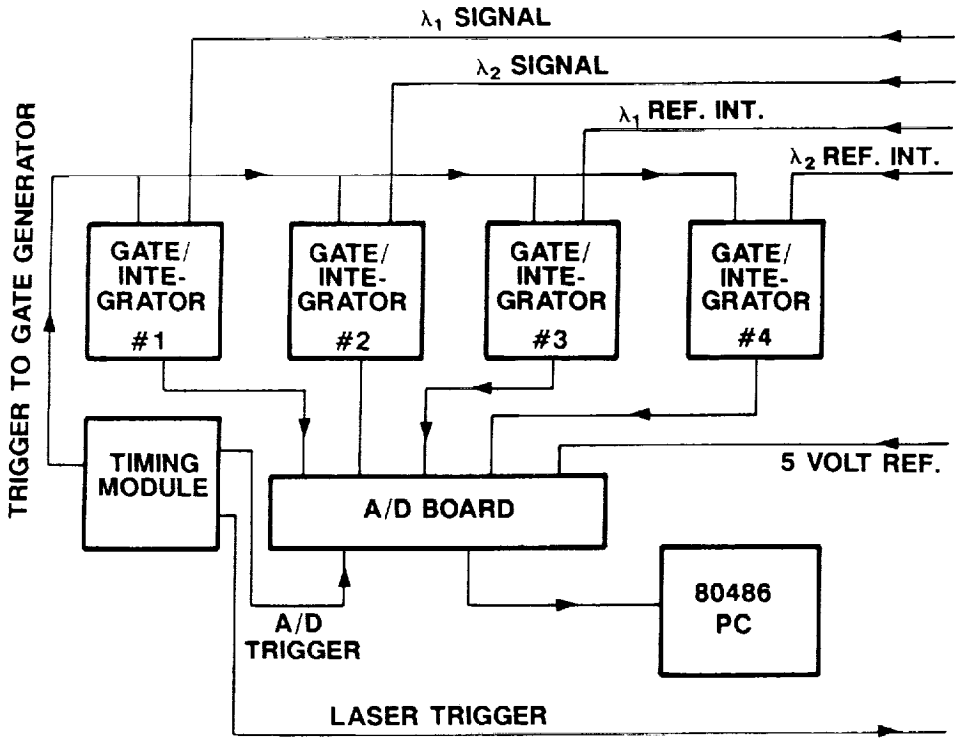

2. Electronic arrangement for the DLDR system

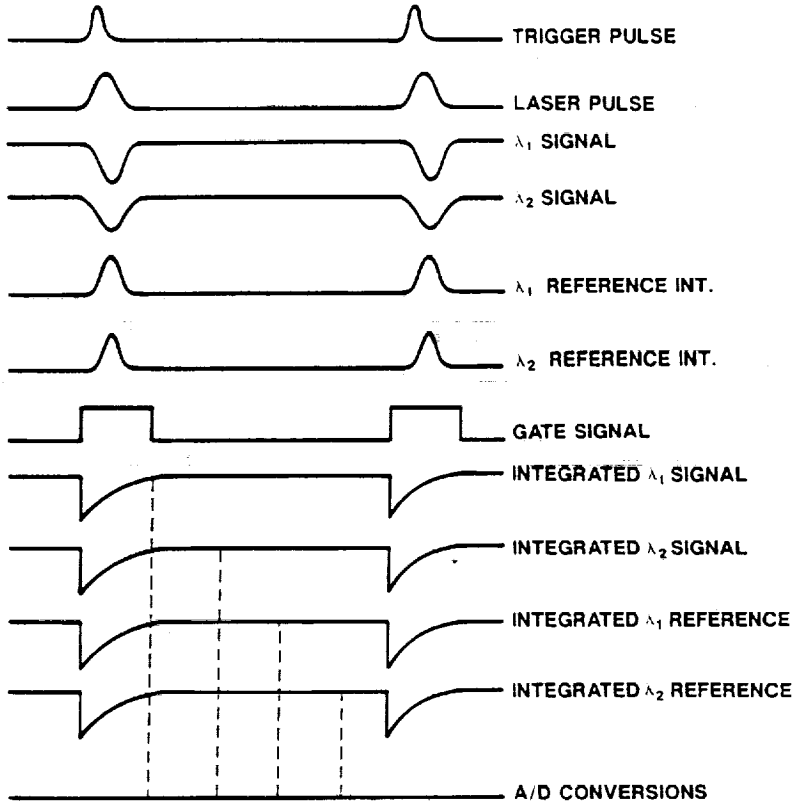

3. Data acquisition procedure

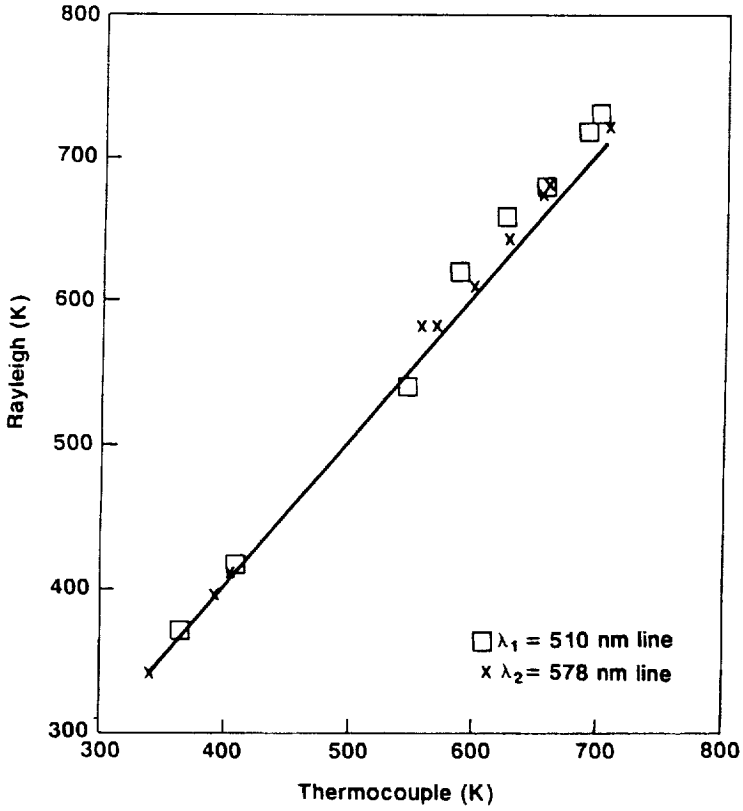

4. Temperature obtained by Rayleigh scattering and thermocouple

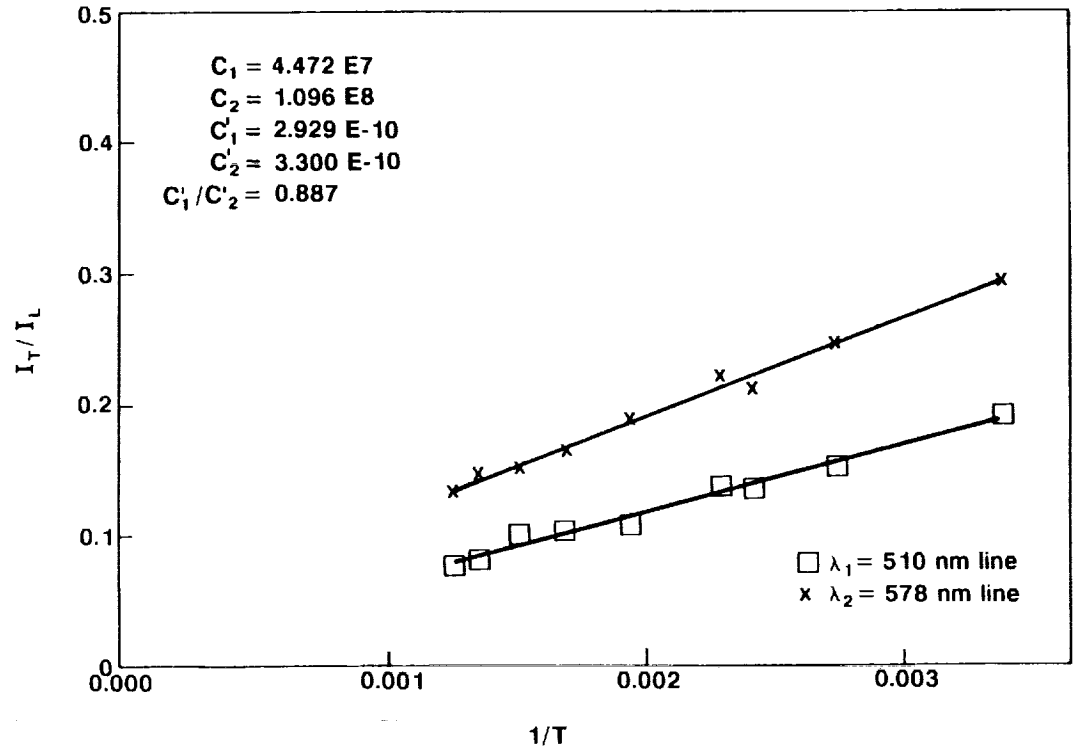

a

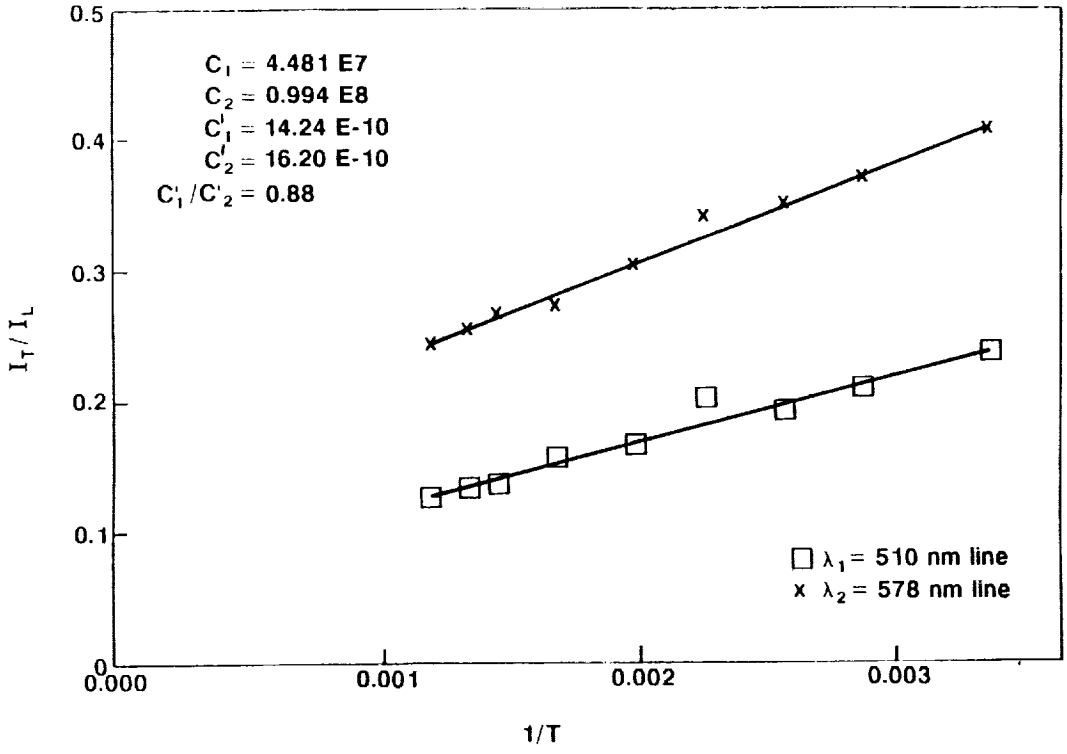

b

5. Calibration curves with various levels of background contamination

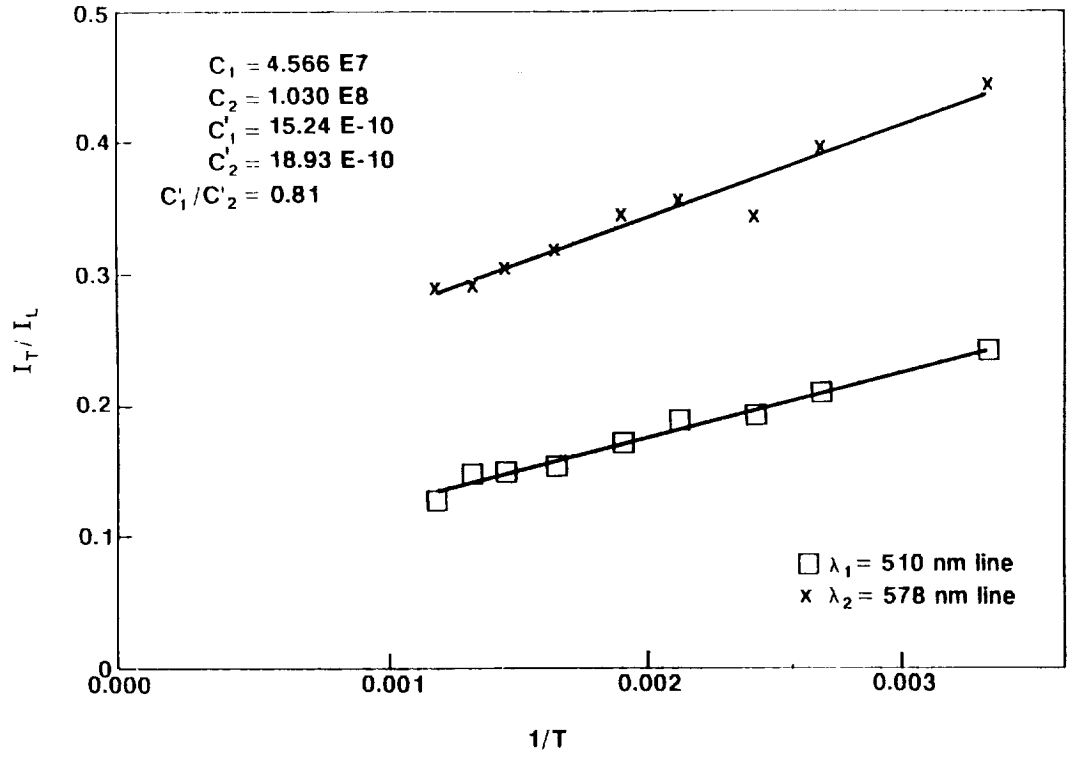

c

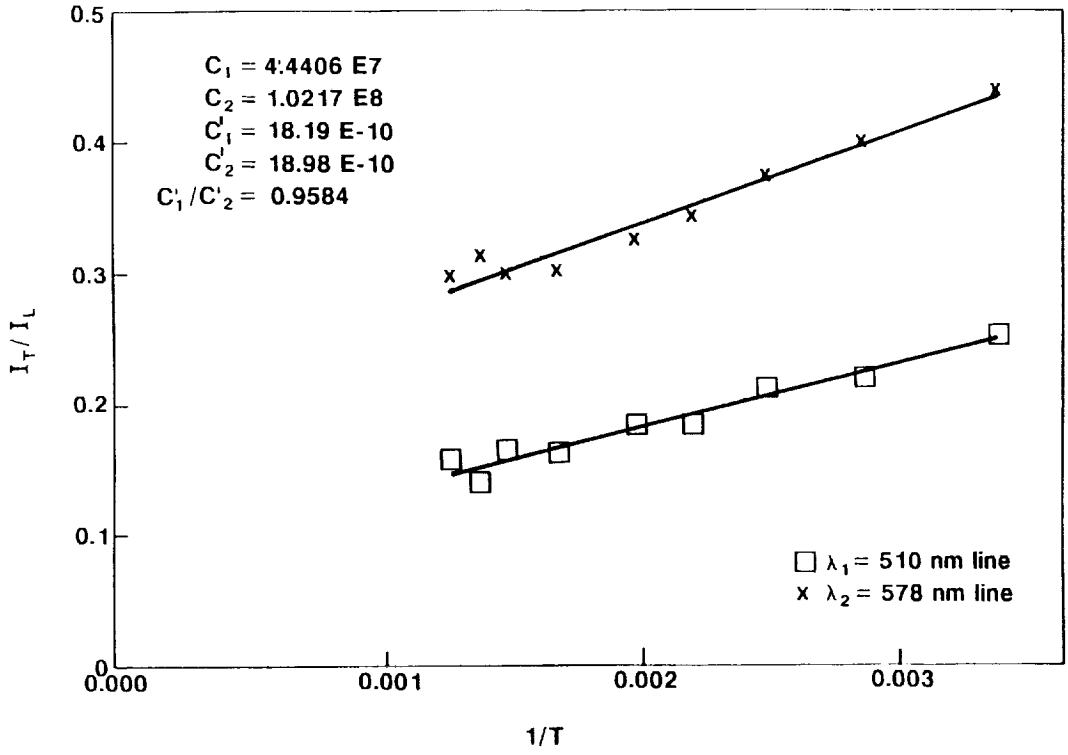

d

5. Calibration curves with various levels of background contamination (cont)

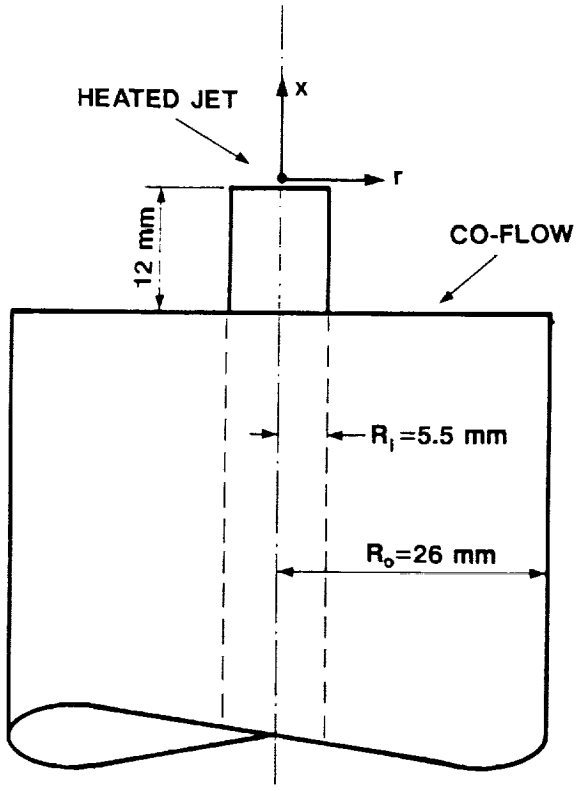

6. Heated jet setup with co-flow

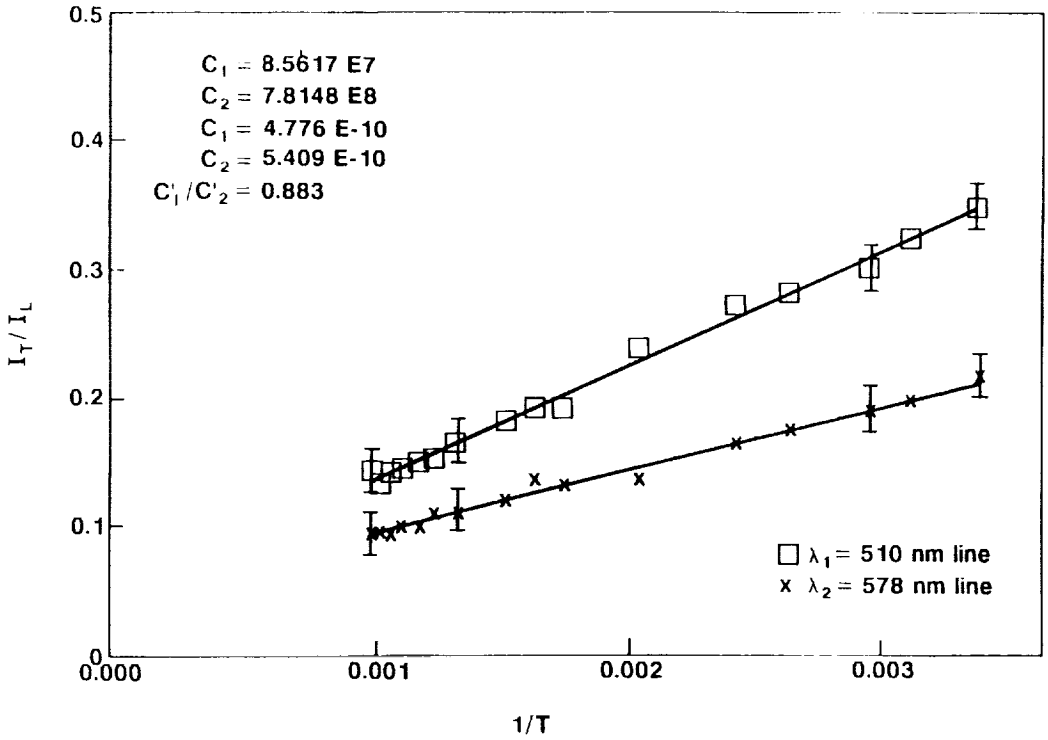

7. Calibration curve for the temperature measurements

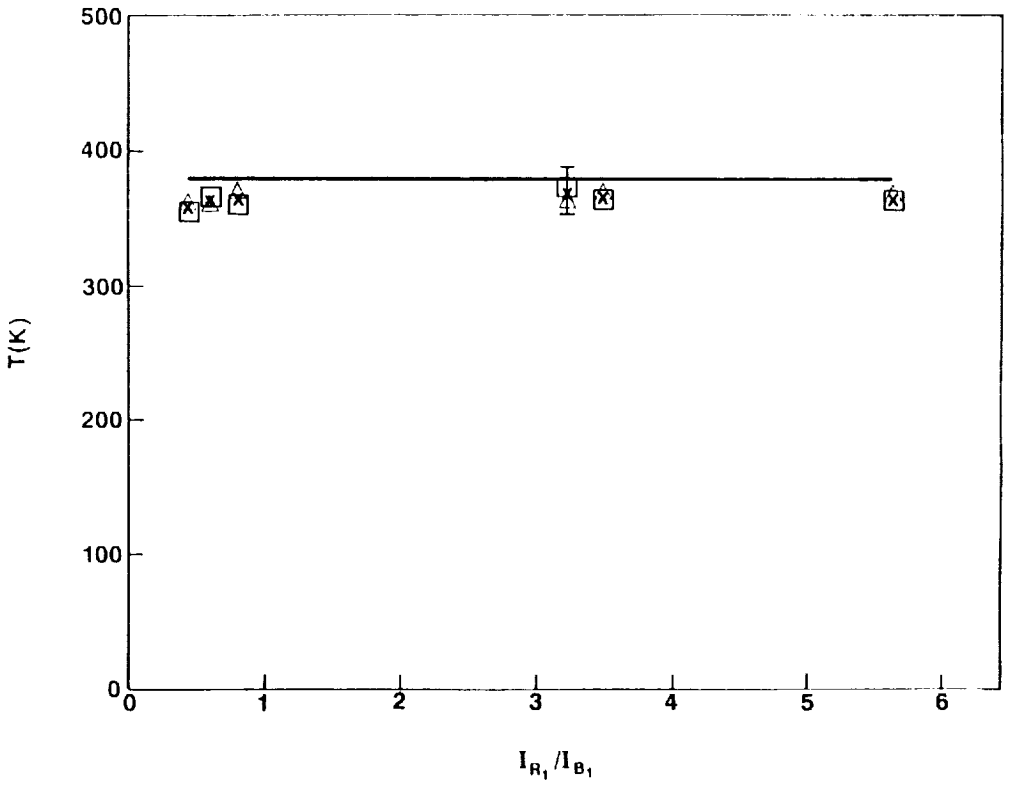

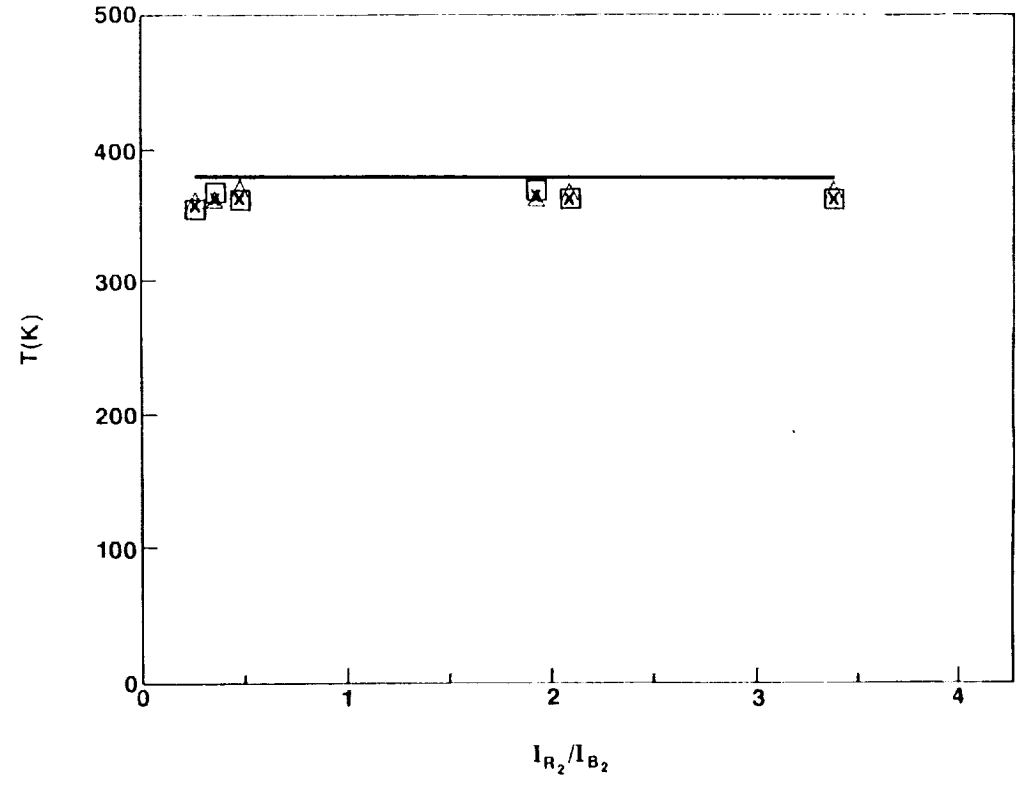

8. Jet temperature measured by the DLDR system (Tjet =380 K).

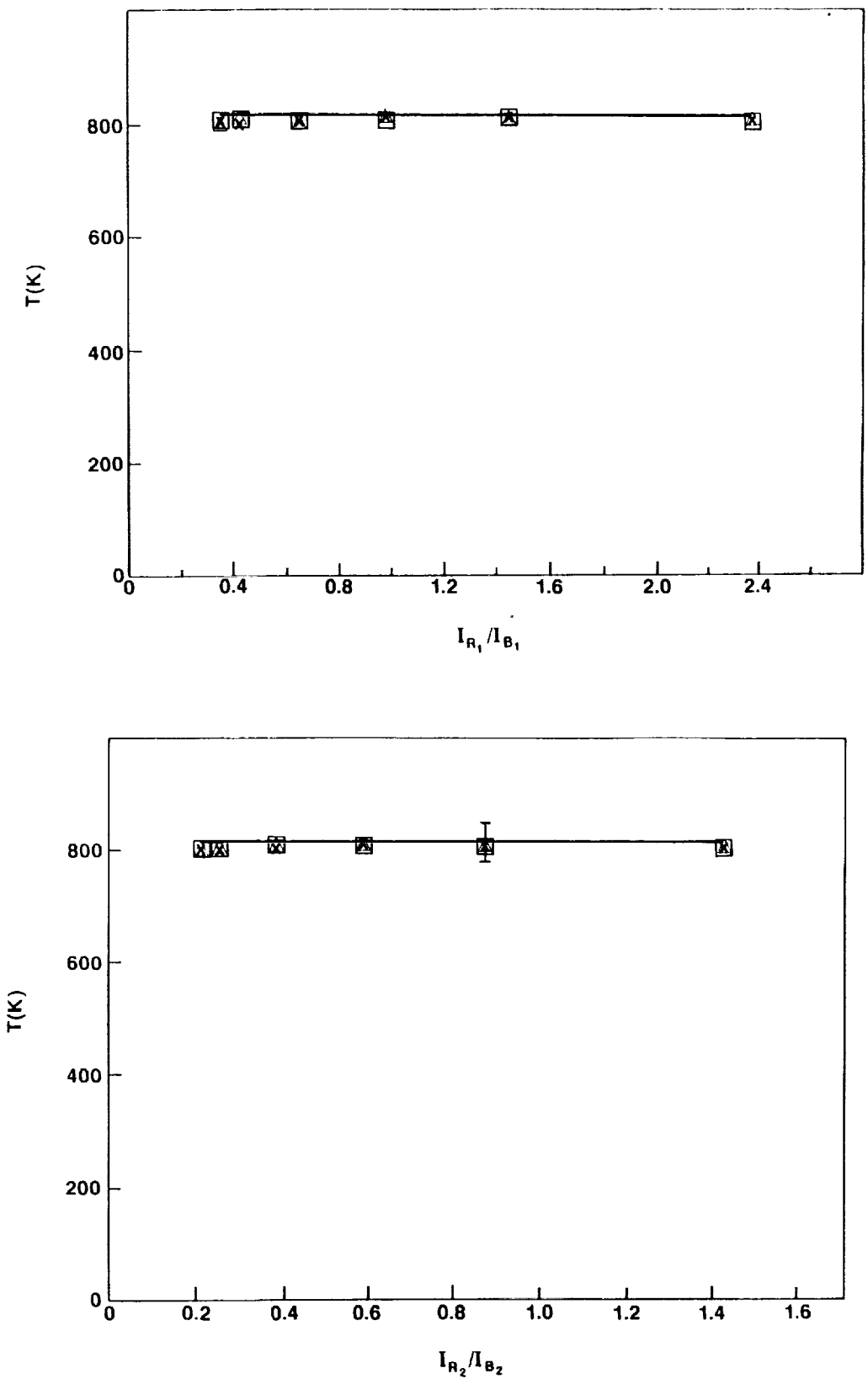

9. Jet temperature measured by the DLDR system (Tjet =805 K).